

Automotive Drum Brake Squeal Analysis Using Complex Eigenvalue Methods

Ibrahim Ahmed¹, Essam Allam², Mohamed Khalil² and Shawki Abouel-seoud³

*(Associate Professor, Automotive Technology Dept., Faculty of Industrial Education, Helwan University, Egypt)

** (Associate Professor, Automotive Engineering Dept., Faculty of Engineering, Helwan University, Egypt)

*** (Professor, Automotive Engineering Dept., Faculty of Engineering, Helwan University, Egypt)

ABSTRACT

Vehicle brakes can generate different kinds of noises. Eliminating brake noise is a very big challenging issue in the automotive industry. Brakes generally develop large and sustained friction-induced oscillations, referred to brake squeal. This brake squeal is considered a serious operational braking problem in passenger cars and commercial vehicles. This paper involves an approach to discover the main causes of drum squeal occurrence using finite element methods (FEM). A modal analysis of a prestressed structure will be performed to predict the onset of drum brake instability. The brake system model is based on the model information extracted from finite element models for individual brake components. An unsymmetric stiffness matrix (MATRIX27) is a result of a friction coupling between the brake lining and drum which may lead to complex eigenfrequencies. This finite element method (FEM) using ANSYS was used to predict the mode shape and natural frequency of the brake system after appropriate verification of FEM. The results showed that changing the contact stiffness of the drum-lining interface play an important role in the occurrence of the squeal. Moreover, decreasing the lining coefficient of friction lead to decreasing the occurrence of the squeal. It showed also that both the frequency separation between two systems modes due to static coupling and their associated mode shapes play an important role in mode merging. It was noted that squeals are most likely to occur when the eigenvectors and eigenvalues of the brake drum and shoes are close to the coupled vibration frequency to confirm that the coupling between different modes was necessary to form instabilities.

The results confirmed that the eigenvectors of the leading and trailing brake shoes are independent from each other with the same natural frequency.

Keywords - Drum, shoe, lining, coupling, natural frequency, instability, modal analysis and finite element.

I. INTRODUCTION

Brake squeal noise is considered a serious braking problem in passenger cars and commercial vehicles. This brake squeal noise has been researched and studied for decades and has not been fully solved yet for either drum or disc brakes. However, the squealed brake is more efficient than the non-squealed one. In particular, buses brake noise is a very serious due to that it is a major source of environmental noise pollution in big cities. Drum brake squeal noise is a complex vibration problem that has coupled vibrations, the sources of which are extremely difficult to be discovered [1]. The nature of the noise that is not repeatable at a given braking condition makes it very difficult to investigate the noise on either the real vehicle or dynamometer in terms of correlating the factors influencing the noise such as pressure, speed, and temperature.

Over the years, drum and disc brake noise have been given various names in an attempt to provide some definitions of the sound emitted such as grind, grunt, moan, groan, squeak, squeal and wire brush [2]. In general, brake noise has been divided into three categories, in relation to the frequency of noise occurrence. The three categories presented are low frequency noise, low-frequency squeal, and high-frequency squeal. Low-frequency noise of drum and disc brake is typically occurs in the frequency range

between 100 and 1000 Hz. Typical noises that reside in this category are grunt, groan, grind, and moan. This type of noise is caused by friction material excitation at the drum or rotor and lining interface. Low-frequency squeal is generally classified as a noise having a narrow frequency bandwidth in the frequency range above 1000 Hz, but below the first in-plane mode of the brake. The failure mode for this category of squeal can be associated with frictional excitation coupled with a phenomenon referred to as “modal locking” of brake corner components. Modal locking is the coupling of two or more modes of various structures producing optimum conditions for brake squeal [2].

High-frequency brake squeal is defined as a noise, which is produced by friction induced excitation imparted by coupled resonances (closed spaced modes) of the rotor or drums itself as well as other brake components. It is typically classified as squeal noise occurring at frequencies above 5 kHz. Since it is a range of frequency, which affects a region of high sensitivity in the human ear. High-frequency brake squeal is considered the most annoying type of brake noise. Brake squeal is a concern in the automotive industry that has challenged many researchers and engineers for years. Considerable analytical, numerical and experimental efforts have been spent on this subject, and much physical insight has been gained on how disc and drum brakes may generate squeal, although all the mechanisms have not been completely understood [3].

In recent years, the focus on brake squeal problems has shifted from fundamental theoretical research to more practical and problem-solving oriented efforts. Instead of a simple schematic model, the brake system model tends to include more brake components, and the effects of design parameters on the stability can be investigated. A linear system model was created based on the modal information of the brake components, and a complex eigenvalue analysis was performed to solve the Equations of motion [4]. Guan et al. [5] constructed a coupled linear model including all brake components and identified the substructure modes, which have great influence on the system stability. Chowdhary et al. [6] developed an assumed modes model for squeal prediction of a disc brake, and found that this

parathion between the frequencies is an important factor in determining the onset of flutter-type instability. Ouyang et al. [7] considered the effects of disc rotation, and the friction-induced vibration of the brake was treated as a moving load problem. With the improvement of numerical techniques, Hamabe et al. [8] and Nack [9] directly conducted a complex eigenvalue analysis with a finite element (FE) model of a brake system including the friction force. However, a nonlinear contact analysis was performed to determine the pressure distribution at the friction interface followed by system linearization and a complex modal analysis, using FE analysis [10]. Thus, in their study, the contact stiffness was dependent on local contact pressure.

The finite element method has been applied to the investigation of brake noise [11, 12], through the emphasis has been upon the investigation of drum brake noise. It can provide predictions of the vibration modes of brake components, but coupling between the brake shoe and drum for a full brake assembly model has not been fully developed. Kusano et al. [11] carried out experimental and finite element analysis to analyze the vehicle drum brake noise, using a half-brake model. Modal models representing the dynamic characteristics of the components were described with a limited number of degrees-of-freedom, then nodes on the rotor and pads were coupled through springs of the same stiffness, which were applied over the whole contact area, or normal, and friction forces were applied on the disc without modeling pads [18]. Full three-dimensional models of disc brake were used to predict the natural frequencies of the brake components [12, 13, 14], which were then connected with springs of the same stiffness. The effect of the coupling between the shoe and drum was discussed by Ghesquire and Castel [13, 14]. However, the absence of the friction force has so far been a limitation of finite element simulations of vibration while braking. Introducing friction force to the finite element model makes the stiffness matrix asymmetric. Resulting in a non-conservative system for which eigensolutions are only available in some commercially available finite element analysis programs.

A frictional counter-coupled model can illustrate the principle of drum brake vibration while squealing, as

a kind of self-excited vibration [15-16]. The squeal vibration of drum results from not some nonlinear factors such as negative slope of friction coefficient, i.e. a negative damping effect, but also the interaction between the complex mode and frictional force from sliding drum [17]. If a constant friction coefficient were large enough, the Equations of motion would have eigenvalues with positive real components, which indicates the vibration having a tendency of unlimited increase. It can also be proved by this frictional counter coupled model [15] that progressive wave is another characteristic of the squeal vibration of drum. Up till now, most of researches in the area of brake squeal depend mainly on the 2-dimensional technique and the 3-dimensional technique is still very limited in solving the squeal problems. The main difficulty in 3-dimensional analysis of brake vibration that the movements of shoes are too complicated to be simulated in the 3-dimensional solution by Finite element. However, the mechanisms of squeal have not been understood completely yet, so that it is not easy to establish an accurate finite element model of drum brake squeal, especially in determining some boundary conditions.

The work presented here based on the conclusions in presented papers, aims to investigate the drum brake squeal noise by finite element analysis (FEA). A three dimensional elasticity dynamics model of drum brake is set up, by which the drum vibration while squealing can be investigated more accurately than 2-D model. A pressure-dependent model for the coupling between the brake drum and the shoe and lining assembly is described and used in the modal analysis of the brake assembly. Predicted vibration modes and frequencies are compared with experimental data for a drum brake noise propensity evaluation. The modal analysis of the brake assembly by FEA, using the friction interface model proposed, is found more useful for evaluation of drum brake designs for noise propensity.

II. VALIDATION OF DRUM BRAKE MODEL

An experimental modal testing is performed on the individual drum brake components to evaluate the vibration characteristics and validate the FE model. So, an impulse excitation using an impact hammer is used to obtain natural frequencies and the associated mode shape of the brake components as shown in

Fig. 1. Then, finite element models (FEM) for the brake drum and lining separately are generated as shown in Fig. 2. Each finite element model is validated by performing the modal testing on the real brake component for the free-free condition followed by modal analysis of the FE model. Free boundary conditions are used in this case because it is the easiest way to simulate experimentally.

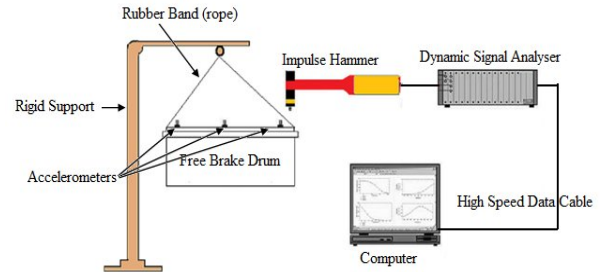


Fig. 1 Modal testing for the free-free brake drum.

As it is well known that, the drum brake assembly consists of five main parts; the drum and the two shoes and linings. The model is created directly using the ANSYS package (FEM). Fig. 2 indicates the meshed drum, shoe, and lining after appropriate simplification to the original parts. A solid45 element has been chosen from the package (ANSYS) library to model the 3-D solid structure that has 8-nodes with three degree of freedom per each node. The drum consists of 11774 brick elements with 18123 nodes, however, the shoe consists of 1260 brick elements with 2666 nodes, and lining contains 2700 brick elements with 2886 nodes. Each lining covers an angle equal to 120° of the drum ring that has an internal diameter of 340 mm as shown in Fig. 3. However, the shoe and shoe rib cover an angle equal to 140° of drum ring that has specifications as shown in Table 1.

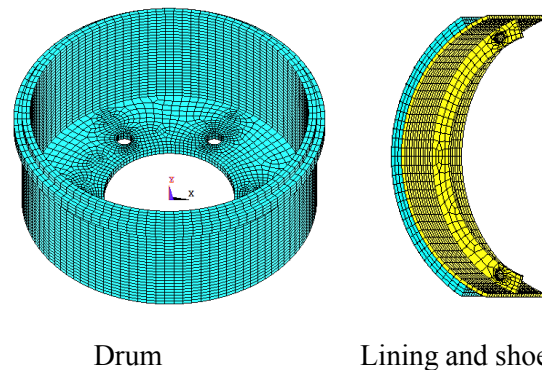


Fig. 2 FEM for the free-free brake drum and lining separately.

In the modal testing shown in Fig. 1, eight accelerometers are mounted along the drum that is hit by an impulse hammer. The tested signal is then fed from the accelerometers to a dynamic signal analyzer and finally to the computer for further analysis. The natural frequencies and modes of the drum and lining were collected in two cases. The first case was a free-free drum and free-free lining however, the second case was the coupled drum-lining with a hydraulic pressure. The collected data has been analyzed in both cases and then the finite element model is being adjusted to control the difference between the experimental results and theoretical results. These natural frequencies data have been collected in Table 1 for comparison.

Each free-free component's FE model is refined and adjusted to make the error as less as possible with experimental modal analysis results [4, 19, 20, 21, and 22]. The accurate simulation of the component models as well as the statically coupled model is important for studying the squeal characteristics either experimentally or analytically by FEM. The brake system's propensity to squeal is very sensitive to the geometry of the system and the material properties. The natural frequencies and mass-normalized mode shapes for each component are extracted from the modal analysis of the FE models. These modal characteristics of the components are used to replace the FE models to form the coupled system, and the total degrees of freedom are greatly reduced. The accuracy of the modal representations of the components and the convergence of the stability analysis results should be checked by ANSYS program.

The boundary conditions have been applied to the drum and shoe, and apply the appropriate solving to the model. Many trials were made to adjust the meshing elements for the drum and shoe with the appropriate number of elements. The lowest difference between the experimental work, and predicted FE model has been achieved in models shown in Fig. 2. These collected data showed a maximum difference of $\pm 3\%$ between the experimental and FEM results for the drum and $\pm 2.5\%$ for the shoe with lining as clear in Table 2. This difference in both cases seems to be acceptable to carry on with these models.

III. COUPLING THE DRUM-LINING FRICTION INTERFACE

As it previously said, the drum brake assembly system consists of five main parts, which are the drum and, leading shoe and trailing shoe. There is a

small gap between the drum and the two shoes during the rotation of the wheel. However, this gap becomes zero at the full contact between the drum and the shoes. The coupling between the brake shoe and lining assembly and the brake drum is made by the contact between them when the brake is actuated and friction force between the lining and drum is generated as shown in Fig. 3. The coupling can be regarded as a "contact stiffness" modeled by springs connecting the brake shoe assembly and the brake drum [11].

However, the model proposed here expects that the contact force between the brake lining and brake drum will determine the degree of coupling, and thus the contact spring stiffness. This means that the contact stiffness over the whole contact area is dependent not only on the brake force applied, but also on the friction interface pressure distribution. The contact stiffness will therefore vary around the contact surface, being higher as the local contact pressure increases. The coupling between the lining and drum can be represented by springs whose stiffnesses represent the local interface contact pressure and the brake shoe can thus be modeled as being coupled to the drum via two springs, one representing the contact stiffness $K_{contact}$ and one representing the brake lining dynamic stiffness K_{lining} [1]. These two springs can then be combined to give a single "coupling" spring whose stiffness is:

$$K_{coupling} = \frac{K_{contact} \times K_{lining}}{K_{contact} + K_{lining}} \quad (1)$$

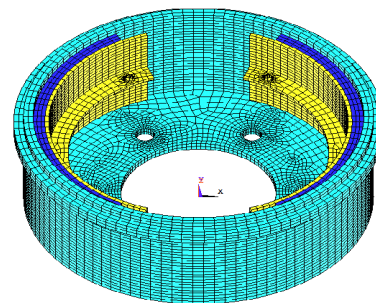
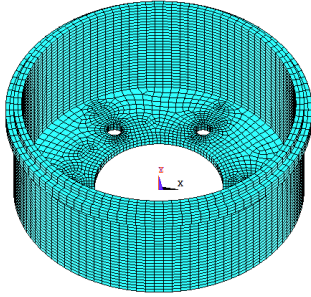
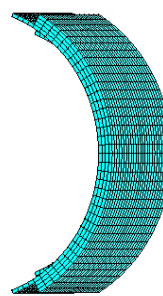


Fig. 3 FEM for the coupled drum brake system assembly.

Table 1 Original brake drum and lining properties and dimensions.

Drum dimensions and properties	Lining and shoe dimensions and properties
Outer drum diameter, 360 mm Inner drum diameter, 340 mm Inner drum cap diameter, 160 mm Outer drum cap diameter, 340 mm Height of drum cap, 10 mm Diameter of holes centerline, 220 mm Height of drum, 150 mm Holes diameter (6), 10 mm Inner diameter of upper ring, 360 mm Outer diameter of upper ring, 360 mm Height of upper ring, 15 mm Density of drum, $7350 \text{ kg} / \text{m}^3$ Young's modulus of drum, $1200 \text{ GN} / \text{m}^2$ Poisson ratio of drum, 0.27	Thickness of lining, 12 mm Width of lining, 120 mm Thickness of shoe, 4 mm Width of shoe, 120 mm Thickness of shoe rib, 4 mm Height of shoe rib, 20 mm Lining arc, 120° Shoe and rib arc, 140° Hole diameter, 10 mm Density of lining, $1350 \text{ kg} / \text{m}^3$ Young's modulus of lining, $200 \text{ MN} / \text{m}^2$ Poisson ratio of lining, 0.23 Density of shoe, $7800 \text{ kg} / \text{m}^3$ Young's modulus of shoe, $2000 \text{ GN} / \text{m}^2$ Poisson ratio of shoe, 0.27

Table 2 Natural frequencies for the modal testing and FE model for free-free brake drum and lining.

Component name	FE	No. of nodes and elements	Mode number	Modal testing (kHz).	FE model (kHz).	Difference
Drum		11774 elements and 18123 nodes	1	1483	1503	1.3 %
			2	1488	1508	1.3 %
			3	2087	2068	-1 %
			4	2140	2200	3 %
			5	2302	2332	1.3 %
			6	2340	2345	0.2 %
			7	2917	2906	-0.4 %
			8	3087	3097	0.3 %
			9	3129	3109	-0.6 %
			10	3203	3253	1.6 %
Lining		Lining 2700 elements and 2886 nodes + Shoe 1260 elements and 2666 nodes	1	1179	1200	2 %
			2	1213	1240	2.5 %
			3	1667	1684	1 %
			4	1843	1820	-1.2 %
			5	2226	2210	-0.7 %
			6	2233	2253	-0.9 %
			7	2605	2600	-0.2 %
			8	2679	2677	0
			9	2861	2886	1 %
			10	3109	3100	-0.3 %

IV. MODELING OF DRUM BRAKE ASSEMBLY.

The steps of creating a linear drum brake assembly model contain three main steps as shown in Fig.4, which are:

- Pre-processor.
- Solution.
- Post-processors.

These three steps include constructing FE models for brake components by ANSYS CAD tools as mentioned previously. A modal analysis technique will be performed to extract the modal eigenvalues and eigenvectors.

Studying the effects of different parameters such as contact and lining stiffnesses and friction forces on the occurrence of squeal incorporating the effects of boundary conditions to form a coupled model.

Fig. 3 shows the finite element model for the coupled drum brake system assembly that contain the main five components which are drum, two shoes and two linings (leading and trailing), participate in the vibrational response of a drum brake system [20-21].

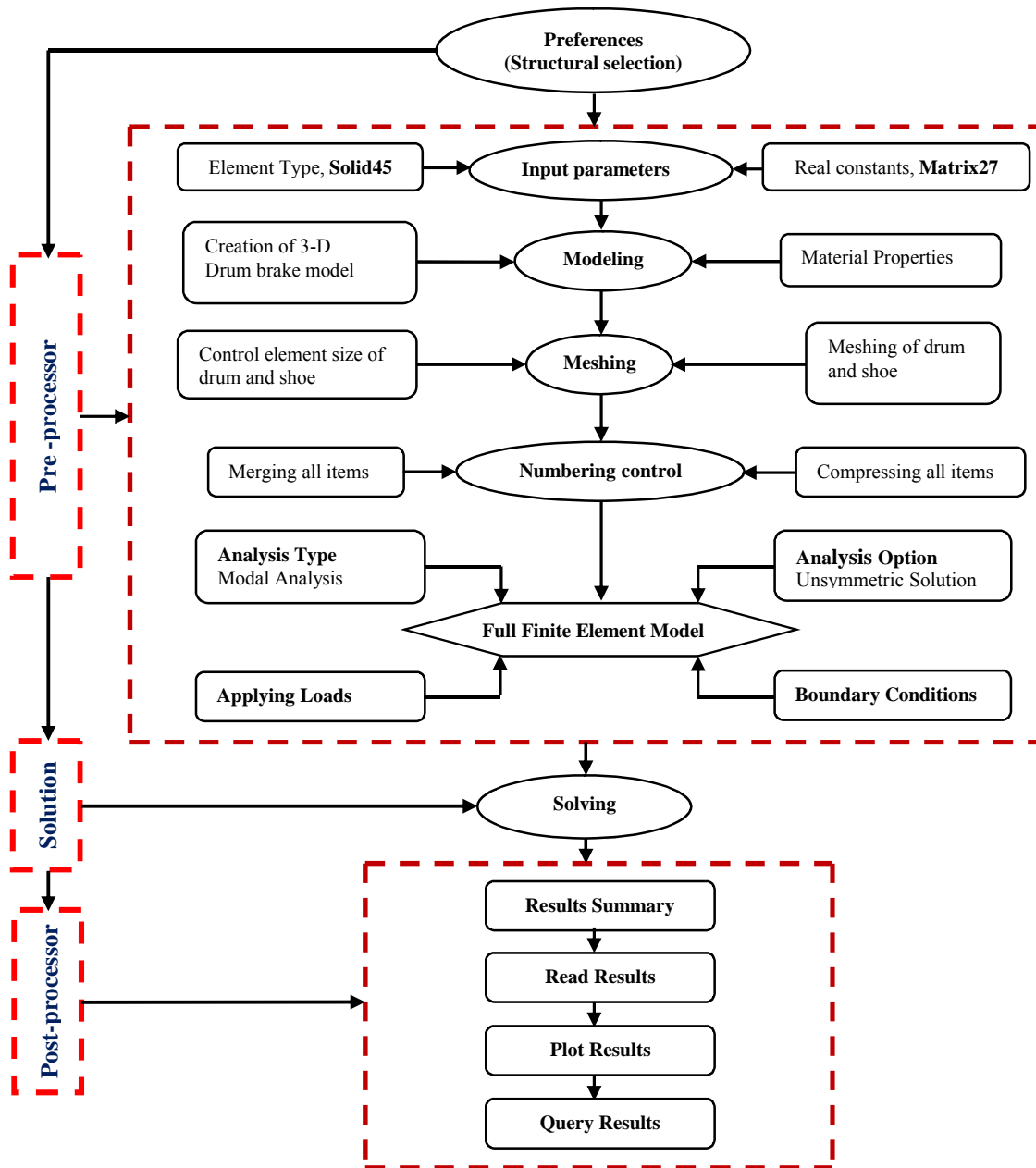


Figure 4 Parametric modeling and modal analysis flowchart.

The attached linings to the shoes will be in contact with the drum during braking to produce the friction forces. These leading and trailing shoes can be moved in different direction opposed to each other through hydraulic cylinders that contain two pistons to assist the shoes in the braking action. It is well-known that the friction-induced vibration is generated by the stiffness and friction coupling between the drum and the shoes through the shoe lining. A simplified coupled model that includes the drum, the shoes, and the shoe lining has been modelled to incorporate the effect of different boundary conditions on the occurrence of squeal as clear in Fig. 5.

Finite Element models of the drum and the shoe with lining separately are built-up by ANSYS package using 3-dimensional brick elements called SOLID45 [24] is clearly shown in Fig. 2. However, the finite element model of the coupled drum brake is shown in Fig. 3. The drum is clamped in the bolt holes (6 holes) positions while the shoe model uses free boundary conditions. The shoe lining is modeled as an integral part of the FE model of the shoe to include the inertial and stiffness influences of the shoe lining on modal characteristics (eigenvalues and eigenvectors) of the shoe.

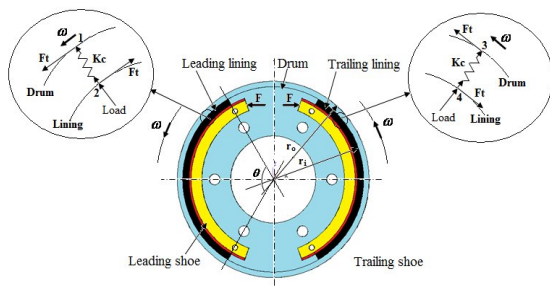


Fig. 5 Schematic diagram of the drum brake assembly showing piston pressure and contact stiffness representation.

The Equations of motion of the uncoupled system including the drum and the identical shoes can be written as [1, 20, 21 and 23]:

$$\{\ddot{q}\} + [\omega^2]\{q\} = \{0\} \quad (2)$$

Where $[\omega^2]$ is a diagonal matrix of the extracted natural frequencies of the components, and $\{q\}$ is an N-vector of generalized coordinates. However, the

number of degrees of freedom of the system, N, is equal to the total number of extracted component modes, [20].

In considering the coupling between the drum and the shoe through the contact lining, the contact interface between the drum and shoe is discretized into a mesh of 2-dimensional contact elements as shown in Fig. 5. The lining material is then modelled as a spring located at the contact elements as mentioned previously. The Equation of motion of the coupled system can be written as follows [20-21];

$$\{\ddot{q}\} + [[\omega^2] + [A] + \mu[B] + [C]]\{q\} = \{0\} \quad (3)$$

Where, [A] and [C] are stiffness contribution due to the lining and shoe supports respectively and [B] arises from friction coupling between the shoes and drum which is asymmetric. In the absence of lining coupling i.e., [A] and μ equal to zero, the eigenvalues are purely imaginary that is being the natural frequencies of the drum components and the shoes coupled through the hydraulic cylinder stiffness and backing plate stiffness. The solution of the Equation 3 gives the eigenvalues of:

$$S = \sigma_i \pm j\omega_i \quad (4)$$

However; in the presence of the lining stiffness coupling but without friction coupling, the eigenvalues are again purely imaginary and correspond to the natural frequencies of an engaged brake system which is not rotating. This is referred to what is called statically coupled system.

In the presence of the lining stiffness coupling but with friction coupling and the [B] is non-symmetric. When all of the eigenvalue are purely imaginary, these correspond to the natural frequencies of an engaged and rotating system. If any of the eigenvalues is complex, it will appear in the form of complex conjugate pairs, one with positive real part and the other with negative real part. The existence of complex roots with positive real parts indicates the presence of mode merging or what is called coupled mode, instability, which causes the brake to squeal. The value of friction coefficient that demarcates stable and unstable oscillations will be referred as a critical value of friction coefficient μ_{cr} . The imaginary part of the eigenvalues with a doublet root

at this μ_{cr} is the squeal frequency and the corresponding mode of the complex structure is the mode shape at this squeal frequency, [20-21].

V. COMPLEX EIGENVALUE ANALYSIS.

The complex eigenvalue analysis technique that is available in ANSYS package is used to determine the stability of drum brake assembly. The real and imaginary parts of the complex eigenvalues are responsible for the degree of instability (unstable frequencies and unstable modes) of the drum brake assembly and are thought to imply the likelihood of squeal occurrence. The importance of this method lies in the asymmetric stiffness matrix that is derived from the contact stiffness and the friction coefficient at the drum-lining interface [14]. In order to perform the complex eigenvalue analysis using ANSYS, four main steps are required [15]. They are given as follows:

1. Nonlinear static analysis for applying drum brake-line pressure.
2. Nonlinear static analysis to impose rotational velocity on the drum.
3. Normal mode analysis to extract natural frequency of undamped system.
4. Complex eigenvalue analysis that incorporates the effect of friction coupling.

In this analysis, the complex eigenvalues using ANSYS are solved using the unsymmetric method. The Equation of motion of any vibrating system is:

$$[M]\{\ddot{u}\} + [C]\{\dot{u}\} + [K]\{u\} = \{F\} \quad (5)$$

Where M, C and K are mass, damping and stiffness matrices, respectively, and u is the generalized displacement vector. For friction induced vibration, it is assumed that the forcing function F is mainly contributed to by the variable friction force at the drum-lining interface. The friction interface is modelled as an array of friction springs as shown in Fig. 5. With this simplified interface model, the force vector becomes linear:

$$F = [K_f]\{u\} \quad (6)$$

Where $[K_f]$ is the friction stiffness matrix. A homogeneous Equation is the obtained by combining

Equations 5 and 6 and by moving the friction term to the left hand side as follows:

$$[M]\{\ddot{u}\} + [C]\{\dot{u}\} + [K - K_f]\{u\} = \{0\} \quad (7)$$

Equation 7 is now the Equation of motion for a free vibration system with a pseudo forcing function in the stiffness term. The friction stiffness acts as the co-called “direct current” spring [23] that causes the stiffness matrix to be asymmetric.

The unsymmetric method, which also uses the full [K] and [M] matrices, is meant for problems where the stiffness and mass matrices are unsymmetric. It uses Lanczos algorithm, Theory Manual [24] that calculate complex eigenvalues and eigenvectors for any system. Matrix27 represented an arbitrary element whose geometry was undefined but whose elastic kinematics response could be specified by stiffness, damping, or mass coefficients. This element matrix27 was assumed to relate two nodes, each with six degrees of freedom per node: translations in the nodal x, y, and z directions and rotations about the nodal x, y, and z-axes as shown in Fig. 5. The stiffness, damping, or mass matrix constants were input as real constants. All matrices generated by this element were 12 by 12. The degrees of freedom were ordered as UX, UY, UZ, and ROTX, ROTY, ROTZ for node 1 followed by the same for node 2 on the leading shoe and also for node 3 and node 4 on the trailing shoe. If one node was not used, so all rows and columns related to this node would be defaulted to zero.

For most brake design, including this study, there was no viscous damping present. According to the geometric instability, variable frictional forces, due to variable normal forces, caused brake squeal to occur [4]. The matrix Equation 5 in the absence of viscous damping and including the frictional forces can be rewritten to be in the form of:

$$[M]\{\ddot{U}\} + [K]\{U\} = \{F_f\} \quad (8)$$

To allow variable normal forces at the drum-lining interface, adjacent nodes on the drum and lining interface were connected together with stiff spring as shown in Figure 5. Since squeal typically occurred at low applying pressures, a constant contact pressure

was assumed between both lining material surface and the drum surface [4 and 26]. As the connected nodes moved towards or away from each other, the magnitude of the normal force increased or decreased according to moving direction. So, the resulting variable frictional forces were written in terms of relative displacement between the mating surfaces as in Equation 6. The matrix, which related the frictional forces to nodal displacement called the frictional stiffness matrix $[K_f]$ or the friction matrix. To obtain a homogeneous Equation, the forces were moved from the right side of Equation 8 to the left side of the same Equation to be in the form of;

$$[M]\{\ddot{U}\} + [K - K_f]\{U\} = 0 \quad (9)$$

The complementary solution to the homogeneous, second order, matrix differential Equation 9 is in the form of:

$$\{U\} = \{\phi\}e^{st} \quad (10)$$

Where

s is the eigenvalue.

$\{\phi\}$ is the eigenvector.

And by substitution in Equation 9 So;

$$([M]S^2 + [K - K_f])\{\phi\} = \{0\} \quad (11)$$

The eigenvalue and possibly the eigenvectors of Equation 11 were complex numbers. Complex numbers contained two parts; real and imaginary parts. For this drum brake system, the eigenvalues always occurred in complex conjugate pairs. For certain mode, the eigenvalue was:

$$S = \sigma_i \pm j\omega_i \quad (12)$$

where σ_i is the real part and represented the natural frequency of the system. However; ω_i is the imaginary part and represented the instability of the system.

A positive damping coefficient causes the amplitude of oscillations to increase with time. Therefore the system is not stable when the damping coefficient is positive. By examining the real part of the system eigenvalues the modes that are unstable and likely to produce squeal are revealed. In another definition of the damping ratio, which is defined as $-2\sigma / |\omega|$.

If the damping ratio is negative, the system becomes unstable, and if the damping ratio is positive, the system becomes stable.

The first unsymmetric MATRIX27 that has been generated between node 1 and node 2, will be performed as a real constant between the drum and the leading shoe as shown in Fig. 5.

$$\begin{bmatrix} F_{X1} \\ F_{Y1} \\ F_{Z1} \\ M_{X1} \\ M_{Y1} \\ M_{Z1} \\ F_{X2} \\ F_{Y2} \\ F_{Z2} \\ M_{X2} \\ M_{Y2} \\ M_{Z2} \end{bmatrix} = \begin{bmatrix} 0 & 0 & \mu \cdot \sin\theta \cdot K_C & 0 & 0 & 0 & 0 & 0 & -\mu \cdot \sin\theta \cdot K_C & 0 & 0 & 0 \\ 0 & 0 & \mu \cdot \cos\theta \cdot K_C & 0 & 0 & 0 & 0 & 0 & -\mu \cdot \cos\theta \cdot K_C & 0 & 0 & 0 \\ 0 & 0 & K_C & 0 & 0 & 0 & 0 & 0 & -K_C & 0 & 0 & 0 \\ 0 & 0 & 0 & 0 & 0 & 0 & 0 & 0 & 0 & 0 & 0 & 0 \\ 0 & 0 & 0 & 0 & 0 & 0 & 0 & 0 & 0 & 0 & 0 & 0 \\ 0 & 0 & 0 & 0 & 0 & 0 & 0 & 0 & 0 & 0 & 0 & 0 \\ 0 & 0 & -\mu \cdot \sin\theta \cdot K_C & 0 & 0 & 0 & 0 & 0 & \mu \cdot \sin\theta \cdot K_C & 0 & 0 & 0 \\ 0 & 0 & -\mu \cdot \cos\theta \cdot K_C & 0 & 0 & 0 & 0 & 0 & \mu \cdot \cos\theta \cdot K_C & 0 & 0 & 0 \\ 0 & 0 & -K_C & 0 & 0 & 0 & 0 & 0 & K_C & 0 & 0 & 0 \\ 0 & 0 & 0 & 0 & 0 & 0 & 0 & 0 & 0 & 0 & 0 & 0 \\ 0 & 0 & 0 & 0 & 0 & 0 & 0 & 0 & 0 & 0 & 0 & 0 \\ 0 & 0 & 0 & 0 & 0 & 0 & 0 & 0 & 0 & 0 & 0 & 0 \end{bmatrix} \times \begin{bmatrix} X_1 \\ Y_1 \\ Z_1 \\ \theta_{X1} \\ \theta_{Y1} \\ \theta_{Z1} \\ X_2 \\ Y_2 \\ Z_2 \\ \theta_{X2} \\ \theta_{Y2} \\ \theta_{Z2} \end{bmatrix}$$

However, the second unsymmetric MATRIX27 that has been generated between node 3 and node 4, will be performed as a real constant between the drum and the trailing shoe as clear in Fig. 5.

$$\begin{bmatrix} F_{X3} \\ F_{Y3} \\ F_{Z3} \\ M_{X3} \\ M_{Y3} \\ M_{Z3} \\ F_{X4} \\ F_{Y4} \\ F_{Z4} \\ M_{X4} \\ M_{Y4} \\ M_{Z4} \end{bmatrix} = \begin{bmatrix} 0 & 0 & -\mu \cdot \text{Sin}\theta \cdot K_C & 0 & 0 & 0 & 0 & 0 & \mu \cdot \text{Sin}\theta \cdot K_C & 0 & 0 & 0 \\ 0 & 0 & -\mu \cdot \text{Cos}\theta \cdot K_C & 0 & 0 & 0 & 0 & 0 & \mu \cdot \text{Cos}\theta \cdot K_C & 0 & 0 & 0 \\ 0 & 0 & K_C & 0 & 0 & 0 & 0 & 0 & -K_C & 0 & 0 & 0 \\ 0 & 0 & 0 & 0 & 0 & 0 & 0 & 0 & 0 & 0 & 0 & 0 \\ 0 & 0 & 0 & 0 & 0 & 0 & 0 & 0 & 0 & 0 & 0 & 0 \\ 0 & 0 & 0 & 0 & 0 & 0 & 0 & 0 & 0 & 0 & 0 & 0 \\ 0 & 0 & \mu \cdot \text{Sin}\theta \cdot K_C & 0 & 0 & 0 & 0 & 0 & -\mu \cdot \text{Sin}\theta \cdot K_C & 0 & 0 & 0 \\ 0 & 0 & \mu \cdot \text{Cos}\theta \cdot K_C & 0 & 0 & 0 & 0 & 0 & -\mu \cdot \text{Cos}\theta \cdot K_C & 0 & 0 & 0 \\ 0 & 0 & -K_C & 0 & 0 & 0 & 0 & 0 & K_C & 0 & 0 & 0 \\ 0 & 0 & 0 & 0 & 0 & 0 & 0 & 0 & 0 & 0 & 0 & 0 \\ 0 & 0 & 0 & 0 & 0 & 0 & 0 & 0 & 0 & 0 & 0 & 0 \\ 0 & 0 & 0 & 0 & 0 & 0 & 0 & 0 & 0 & 0 & 0 & 0 \end{bmatrix} \times \begin{bmatrix} X_3 \\ Y_3 \\ Z_3 \\ \theta_{X3} \\ \theta_{Y3} \\ \theta_{Z3} \\ X_4 \\ Y_4 \\ Z_4 \\ \theta_{X4} \\ \theta_{Y4} \\ \theta_{Z4} \end{bmatrix}$$

VI. PREDICTED RESULTS OF THE FINITE ELEMENT AND DISCUSSIONS.

The results herein represent the described FEM of drum brake system as shown in Fig. 3 that its dimensions and properties are given in Table 1 and be validated as discussed previously. A total number of 100 modes were extracted through ANSYS by coupling of the drum brake items in the frequency range 1-15 kHz (squeal range). These modes include different modes of the drum and the two shoes separately as shown in Figs 6, 7, 8 and 9. These modes include six rigid body modes for each shoe, modes up to the natural frequency of 7366 Hz for the shoes, and non-rigid body modes up to frequency of 14859 Hz for the drum. However, for the coupled modes, it gives frequencies up to 5094 Hz. Figs 6 and 7 show a sample of selected drum modes and displacement contour equivalent at each mode.

The first mode occurred at 1482 Hz with 4 nodal lines as shown clearly in Fig. 6-a and five nodal lines at frequency 2302 Hz as clear in Fig. 6-b. A mix of 6, 7, 8 and 9 nodal lines appear clearly in Fig. 6-c, d, e and f that have been reached in FEM free-free drum.

Fig. 7 shows the displacement contour occurred at modes 1, 5, 12, 36, 54 and 64 respectively showing the maximum and minimum displacement that occurred on the drum ring or drum cap due to the in-plane vibrational mode.

Fig. 8 shows some selected shoe modes; which is a combination between the bending mode and twisting mode of the shoe. The modal analysis of the free-free shoe mode includes six non-rigid body modes for each shoe up to natural frequency of 7366 Hz. It showed a mixed of longitudinal bending mode and lateral bending mode as clear in the 1st mode and 11th mode at frequencies of 1179 and 3516 Hz respectively however; a combination of lateral and longitudinal twisting mode that occurred at 6th and 19th modes at frequencies of 2233 and 4383 Hz respectively. Fig. 9 shows some selected displacement contour at modes 1, 2, 6 and 38 showing a maximum and minimum displacement that occurred due to modal analysis of the free-free shoe of the drum brake.

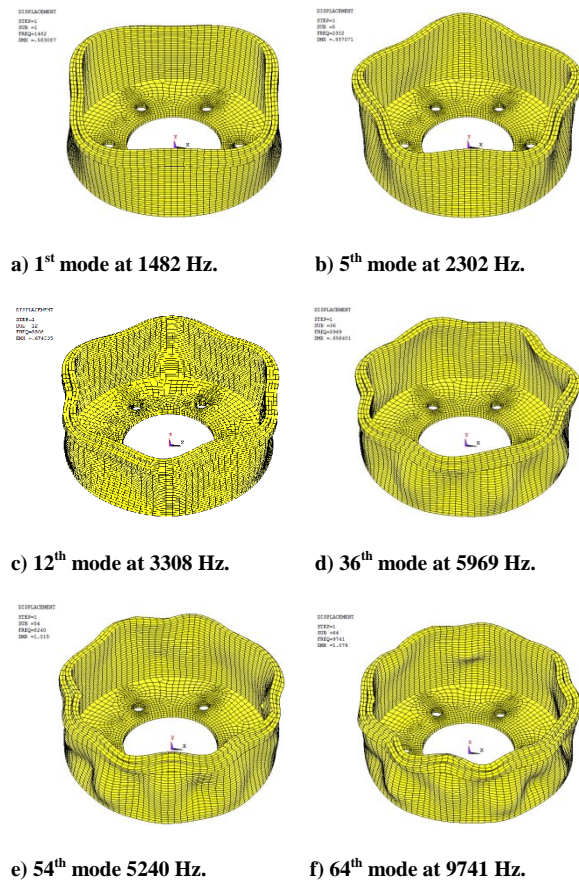


Fig. 6 Sample of selected drum natural frequencies and mode shapes.

A total number of 100 modes were extracted through ANSYS by coupling of the drum brake items in the frequency range 1-15 kHz (squeal range) as mentioned previously. These modes include different modes of the drum and the two shoes separately and combined as shown in Fig. 10. These modes include rigid body and non-rigid body mode for both drum and two shoes up to frequencies of 5094 Hz. Fig. 10 shows a mix of mode nodal lines for the coupled drum brake ranging from 0 to 8 lines which is very clear at modes 5, 11, 14, 33, 37, 61 and 96 respectively. Coupled modes 1 and 2 do not indicate any nodal lines or circumferential circles on the drum ring surface however; it showed a shoe bending mode type at frequencies 1154 and 1218 Hz.

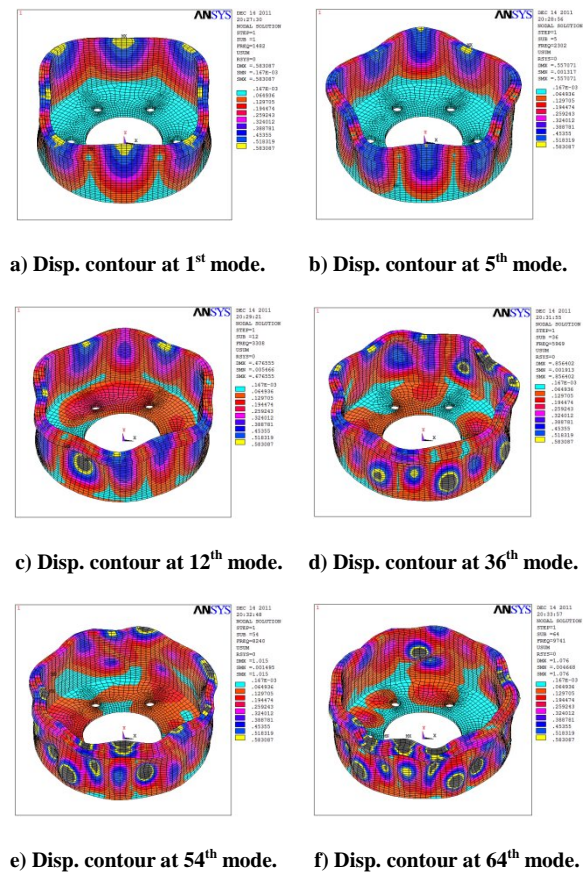


Fig. 7 Displacement contour for selected drum modes.

It showed also the in-plane vibration mode which is clear at the drum hub. The natural frequencies occurred at each component of the drum brake system at 0.42 coefficient friction. It is very clear that the drum modes occur below 5100 Hz. A number of two nodal lines appear in some modes such as 11th and 12th mode as shown in Fig. 10-d and 10-e. However; 3 nodal lines appear in the 33rd mode and 4 nodal lines in the 5th mode as examples of these lines of modes. The number of nodal lines increases with the increase of natural frequency to be 5 nodal lines as shown in 14th mode and 6 nodal lines in the 37th mode. A number of 7 nodal lines appear very rare as shown in Fig. 10-i at 61st mode and the 8 nodal lines appears once in the 96th mode as also shown in Fig. 10-j.

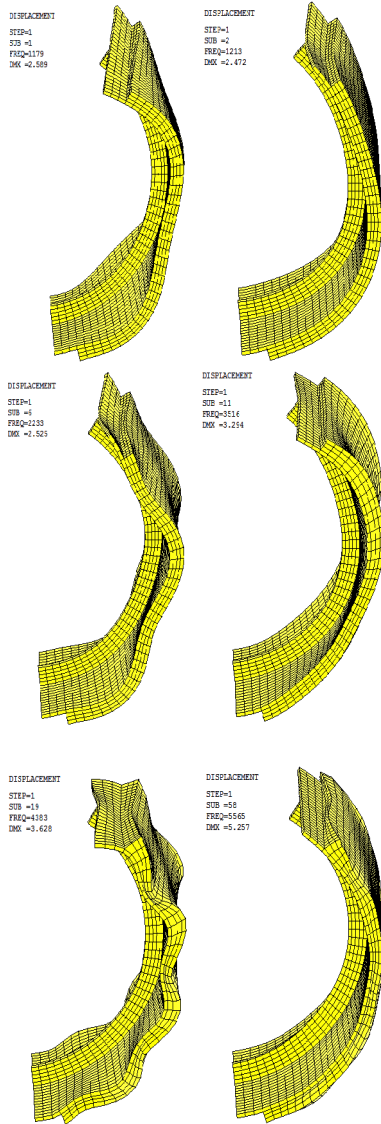


Fig. 8 Sample of selected shoe natural frequencies and mode shapes.

The predicted eigenvalues of the drum brake system at different drum rotating speeds of 0, 10, 20 and 30 rad/sec, whose frequencies are within the measurable frequency range, are presented in Table 3 at moderate friction coefficient of 0.42. The predicted unstable frequencies for the coupled drum brake system are 1154, 1218, 1315, 1458 and 1748 Hz which are the first five natural frequencies.

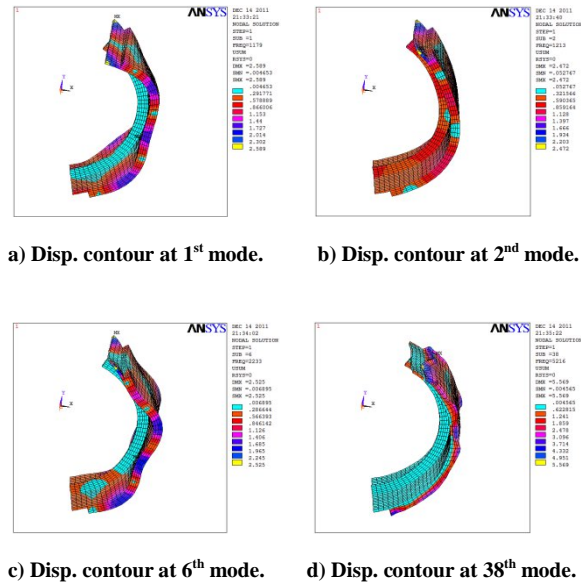


Fig. 9 Displacement contour for selected shoe modes.

Fig. 11 shows some selected displacement contour for the coupled drum brake system at modes 14, 17, 31, 36, 61 and 96 showing a maximum and minimum displacement that occurred due to modal analysis of the coupled system. This figure indicates the vibrating parts of the coupled drum brake such as 17th mode that shows the vibrating trailing shoe. Modes 31st and 61st show the vibrating drum hub (drum cap); however the last 3 modes which are 14, 36 and 96 show the vibrating drum ring.

Fig. 12-a and 12-b show the real part that represents the instabilities of the system when it is positive values or stabilities of the system when it is negative values, against the imaginary part which represents the natural frequencies of the system in the squeal range at 10 and 30 rad/sec of drum rotation. It is realized that as the rotation increase the system seems to be more stable than at a low speeds as clear from figures. It is also realized that the maximum natural frequency of the drum is 5094 Hz occurs at mode 100. However, the maximum natural frequency of the leading shoe is 4940 Hz occurs at mode 91 and the natural frequency of the trailing shoes is 4715 Hz occurs at mode 82 of the coupled drum brake system. The phase angle of this mode is 2°, which equal to phase angle = $\tan^{-1}\left(\frac{\text{Im. Part}}{\text{Re. Part}}\right)$ [24]. When the

two real parts are the same with different signs, it means that they have a phase difference of 180°. It can be clear that the squealing frequency for the leading and trailing occur alternatively between each other. It is very apparent in Figs. 10-a & 10-b that the coupled system is slow below 5 kHz.

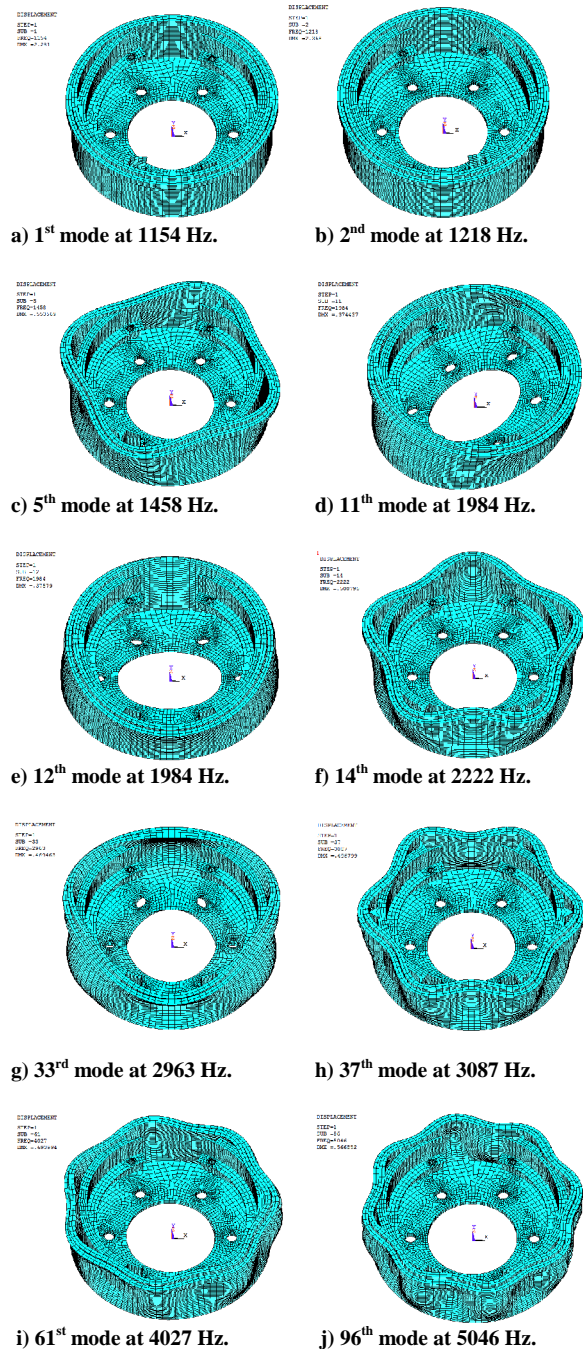


Fig. 10 Sample of selected coupled mode frequencies and modes shapes.

One of the main objectives of this study is to understand the effect of mode merging on the occurrence of brake squeal noise, which is not dependant on the kind of the used brake. The eigenvalue analysis of the drum coupling shown in Equation 3 gives a complex mode that contain two parts, the first part is the real part (instability) and the other part is the imaginary part (natural frequency) as mentioned earlier. The solution of this Equation achieved by substitution with the drum, lining and shoe properties shown in Table 1. Fig.13 shows the variation of the natural frequencies with changing the coefficient of friction in the range (0- 0.8) at the leading and trailing contact stiffness's. It is known that the eigenvalues and eigenvectors change when friction coefficient varies. At the critical value of friction coefficient μ_{cr} , a pair of modes merge, i.e., their frequencies and mode shapes become identical. This merging condition describes the onset of squeal very clearly [25], as seen in Fig. 13.

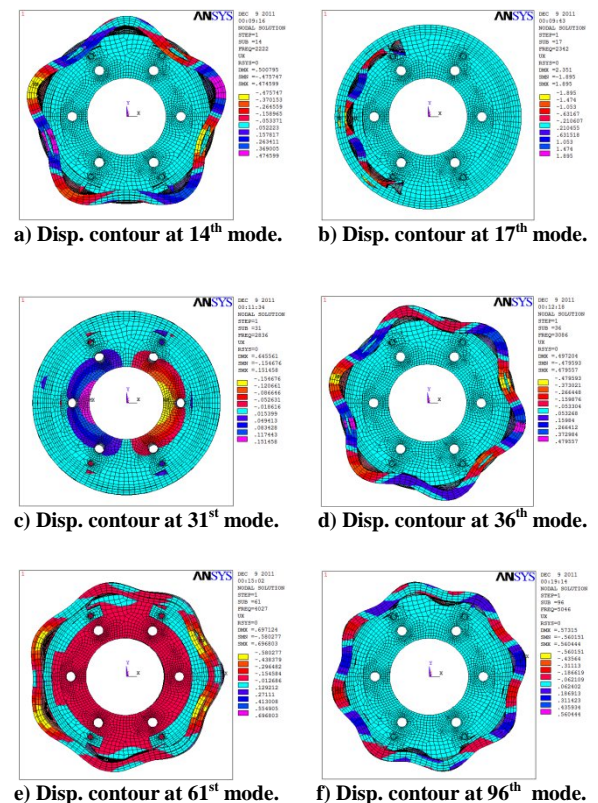


Fig. 11 Displacement contour for selected coupled modes.

The mode-merging instability due to leading-drum coupling occurs four times during this coupling in the frequency range 1-15 kHz at friction coefficients of (0-0.8) and leading contact stiffness of 200 MN/m as shown in Fig. 13-a. The first mode merging occurs between modes 1 & 2 at $\mu = 0.22$ with a torsional mode shape and this friction coefficient called critical friction coefficient μ_{cr} .

bending mode shapes and a natural frequency near to 4150 Hz. The last mode merging occurs between 94th and 95th modes at $\mu_{cr} = 0.71$ with a combination of torsional and bending mode shape and a natural frequency close to 5310 Hz.

Table 3 The first five predicted eigenvalues (Hz) of the coupled drum brake.

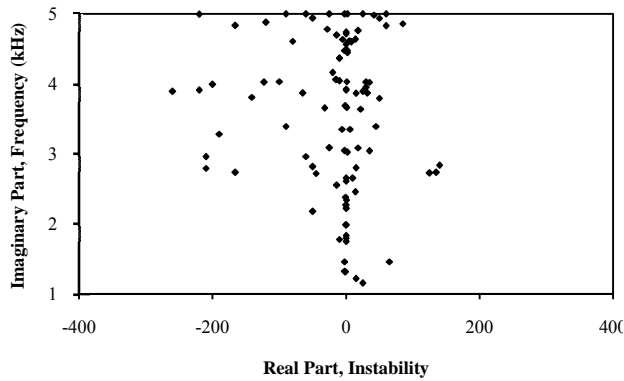
ω rad/sec	S_1	S_2	S_3	S_4	S_5
0	-25±1154	15±1218	-05±1315	0.1±1458	-12±1748
10	-18±1154	-17±1218	1.4±1315	7±1458	1.3±1748
20	2±1154	5±1218	-16±1315	-11±1458	-22±1748
30	-20±1154	-16±1218	-5±1315	0.5±1458	2±1748

It is realized that when μ is bigger than μ_{cr} , the corresponding eigenvalues become complex, its imaginary parts (squeal frequency) near 1218 Hz. The second mode merging occurs between modes 12 and 13 near $\mu_{cr} = 0.58$, with a bending mode shapes and a natural frequency near to 2400 Hz. The third mode merging occurs between 55th and 56th modes near $\mu_{cr} = 0.61$, with a bending mode shapes and a natural frequency near to 4100 Hz. The last mode merging occurs between 94th and 95th modes at $\mu_{cr} = 0.34$ with a combination of torsional and bending mode shape and a natural frequency close to 5094 Hz.

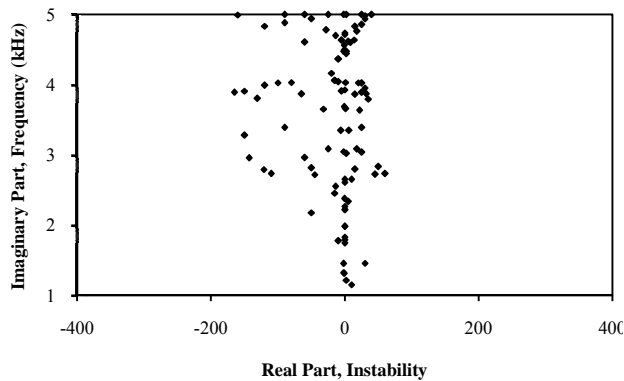
It is found that squeal frequencies are often close to natural frequencies of one or more of the components or near some natural frequencies of the statically coupled system. Since both the frequencies and mode shapes change as the brake is engaged, and further change as the friction is included, it may be difficult to identify which component modes lead to squeal. Moreover, there are many more component modes in a drum brake system, and it is difficult to explain why squeal occurs only at a few frequencies.

However, The mode-merging instability due to trailing-drum coupling occurs also four times during this coupling in the frequency range 1-15 kHz at friction coefficients (0-0.8) and trailing contact stiffness of 150 MN/m as shown in Fig.13-b. The first mode merging occurs between modes 1 and 2 at $\mu = 0.41$ with a torsional mode shape and this friction coefficient called critical friction coefficient μ_{cr} . The corresponding eigenvalues at this merging become complex, its imaginary parts (squeal frequency) near 1225 Hz. The second mode merging occurs between modes 12 and 13 near $\mu_{cr} = 0.15$, with a bending mode shapes and a natural frequency near to 2500 Hz. The third mode merging occurs between 55th and 56th modes near $\mu_{cr} = 0.42$, with a

It is also found that the modes with the least separation due to static coupling tend to merge and become complex for higher values of friction coefficient and that agrees with the fact that usually the neighbouring modes with close frequencies arising due to components symmetry tend to merge, [26]. It can be expected that the shapes of a pair of modes also play an important role in mode merging besides the closeness of their frequencies. For each statically coupled mode for the system at $\mu = 0$, the mode shapes of the two shoes are either identical to each other or differ by a phase angle of 180° as shown clearly in Figs. 10-a and 10-b.



a) Rotation speed of 10 rad/sec.

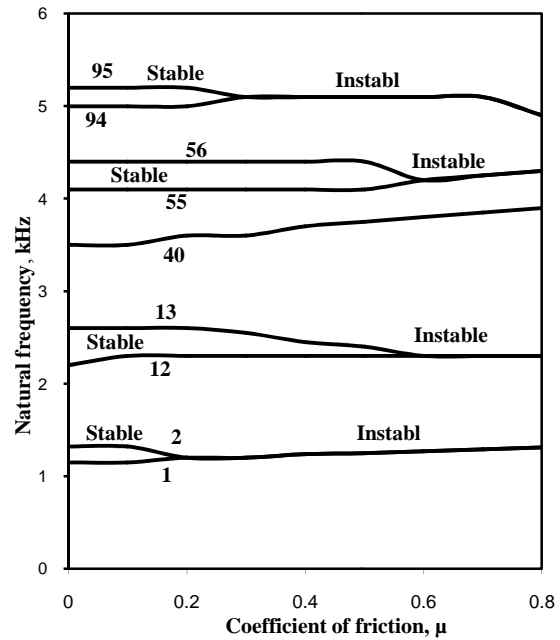


b) Rotation speed of 30 rad/sec.

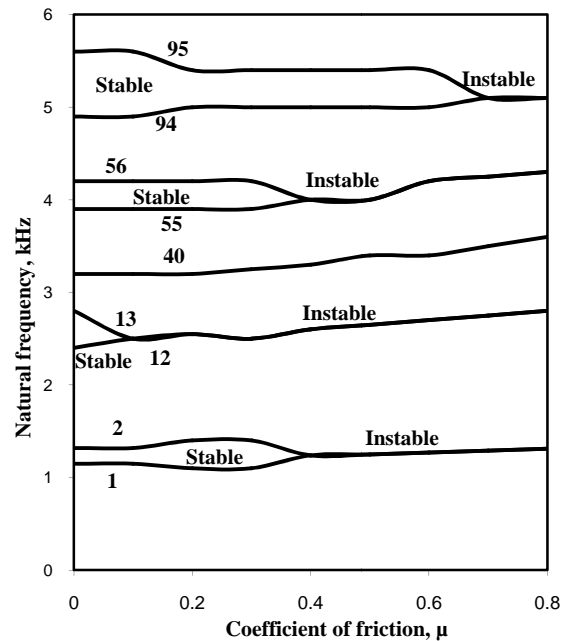
Fig. 12 Real part against Imaginary part of the coupled drum brake system at 10 and 30 rad/sec.

The mode shapes of the shoes show a strong resemblance to those of the corresponding drum side wall where the two are in contact through the lining. The statically coupled modes can be divided into two groups: the first group which the two shoes move in the opposite radial direction (one moves outwards while the other moves inwards) however; the second group which the two shoes move in the same radial direction. All the modes in the same group will be termed "compatible", while the modes from different groups will be termed "incompatible" [20]. Compatible modes are more similar than incompatible modes at it $\mu = 0$ and can quite possibly become identical when μ is increased. Incompatible modes such as mode 40 and mode 55 are never seen

to combine to a merging state even though their frequency separation is quite small at $\mu = 0$.



a) at leading contact stiffness of 200 MN/m.



b) at trailing contact stiffness of 150 MN/m.

Fig. 13 Natural frequency of the system against the Coefficient of friction

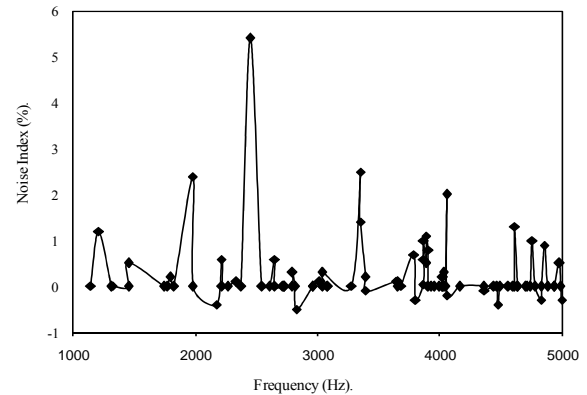
The system can be coupled dynamically by introducing the matrices [B] and [C] shown in Equation 3. These two matrices introduce friction into the system. With the coupled system defined, it is possible to perform stability analyses to determine the conditions on system parameters that lead the brake system into squeal. A standard method of presenting stability is to plot the imaginary components of the eigenvalues (the natural frequencies) as a function of the coefficient of friction at the interface as shown in Figs.13-a, b. When a coupled system becomes unstable, it appears that the strain in the lining is minimized for the unstable modal pair of the drum and shoe. This allows for the greatest energy transfer between the shoe and drum. When the modes are nearly identical the friction force is applying the maximum force possible onto the opposite member. This results in the modal coupling, due to the curved shape of the shoes, being at its maximum value. At the same time, the frictional moment being produced is also at its maximum, thus resulting in a self-excited unstable system.

In terms of noise index (NI), an automotive drum brake system may possess many unstable vibration modes in the audible frequency range. However, not all of them result in squeal. Vibrational modes slightly unstable in the theoretical sense may never become unstable in reality due to dissipative damping in a real drum brake system. To compare the squeal propensity among unstable vibrational modes, the magnitude of the instability has been traditionally employed as a noise index. However, because the instability measurement associated with the high frequency modes are often greater than those of low frequency modes, using the magnitude of the instability as a noise index often implies high frequency squeal is more likely to occur than low frequency squeal. In this study, the noise index was defined as Yuan [28] for each vibration mode;

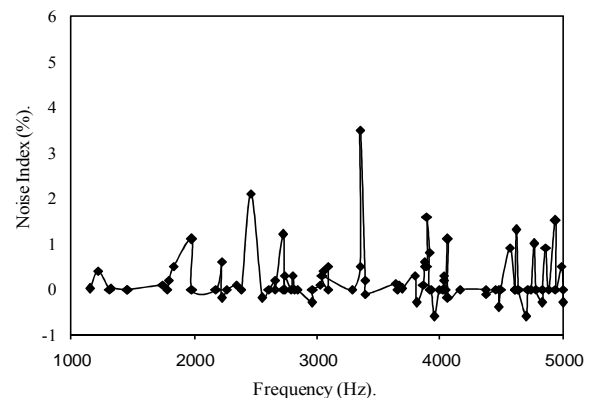
$$\text{Noise Index} = \frac{\sigma_j}{\sqrt{\sigma_j^2 + \omega_j^2}} \times 100 \% \quad (j=1,2,\dots) \quad (13)$$

Where, σ_j is the instability of the system (real part) and ω_j is the natural frequency of the system (imaginary part).

The greater the noise index the more likely the corresponding mode was considered to cause audible squeal noise. It is realized in Figs. 14-a and 14-b that the maximum noise index was 5.4%, which was at frequency 2457 Hz occurred at rotating velocity of 10 rad/sec. However; the maximum noise index of 3.5% occurred at frequency of 3352 Hz at 30 rad/sec. The highest noise indexes were found at the maximum instabilities to confirm that the audible squeal noise could occur at the maximum instabilities as also indicated by Yuan [28].



a) Noise index at rotating velocity of 10 rad/sec.



b) Noise index at rotating velocity of 30 rad/sec.

Fig. 14 the noise Index against the frequency of the coupled drum brake system.

VII. CONCLUSION

The main conclusion from this work can be summarized as follows:

- Brake squeal is a phenomenon of self-excited friction induced vibrations resulting from mode coupling. The eigenvalues and eigenvectors of a coupled drum brake system are able to provide relevant information about the modes involved in brake squeal.
- The modal behaviors components can be extracted from FEM representation of the drum brake system analysis. FE analysis makes it easy to capture geometry complexities of the components and incorporate the results of contact analysis in the system model.
- When the separation between the two modes due to static coupling is small and their mode shapes are compatible, the two modes can merge when the friction is introduced and increased. The instabilities come from the compatible modes when they are identical. So, the mode shapes of brake components most likely are measured with experimental methods has a great on mode merging. The understanding of the important role of mode shapes is expected to be of great help for the prediction of the occurrence of squeal.
- The stability boundaries are sensitive to changes in parameters such as contact stiffness.
- The changes in separations partially reveal the effects of the parameters on system stability and can provide an explanation to some squeal reduction techniques due to the correlation between μ_{cr} values and the separations of the statically coupled frequencies.
- When there is more than one mode with positive real parts of their eigenvalues, the one with the largest real part for the current set of system parameters will be the mode which drives the squeal response. The value of the coefficient of friction at which the dominant mode's eigenvalues merge and become unstable is called the critical value of the coefficient of friction.
- The greater the noise index (NI) the more likely the corresponding mode was considered to cause audible squeal noise.

REFERENCES

- [1] A.J. Day, and S.Y. Kim, Noise and vibration analysis of an S-cam drum brake, Proceedings of Inst. of Mech. Engrs., Vole 210, Part D *Journal of Automobile Engineering*, pp. 35-43, IMechE 1996.
- [2] K.B. Dunlap, M.A. Riehle, and R.E. Longhouse, An investigative overview of automotive disc brake noise, *SAE Paper* 1999-01-0142.
- [3] F. Chen, J. Chern, and J. Swayze, Modal coupling and its effect on brake squeal, *SAE Paper* 2002-01-0922.
- [4] G.D. Liles, Analysis of disc brake squeal using finite element methods, *SAE Paper* No. 891150, 1989.
- [5] D. Guan, and D. Jiang, A study on disc brake squeal using finite element methods, *SAE Paper* No. 980597, 1998.
- [6] H.V. Chowdhary, A.K. Bajaj, and C.M. Krousgrill, An analytical approach to model disc brake system for squeal prediction, *Proceedings of DETC 2001/VIB-21560*, ASME, Pittsburgh, PA, 2001, pp. 1–10.
- [7] H. Ouyang, Q. Cao, J.E. Mottershead, and T. Treyde, Vibration and squeal of a disc brake: modelling and experimental results, *Proceedings of the Institution of Mechanical Engineers, Part D: Journal of Automobile Engineering* 217 (10) (2003) 867–875.
- [8] T. Hamabe, I. Yamazaki, K. Yamada, H. Matsui, S. Nakagawa, and M. Kawamura, Study of a method for reducing drum brake squeal, *SAE Paper* No. 1999-01-0144, 1999.
- [9] W.V. Nack, Brake squeal analysis by finite element, *International Journal of Vehicle Design* 23 (3/4) (2000) 263–275.
- [10] Y.S. Lee, P.C. Brooks, D.C. Barton, and D.A. Crolla, A predictive tool to evaluate disc brake squeal propensity, Part 1: the model philosophy and the contact problem, *International Journal of Vehicle Design* 31 (3) (2003) 289–308.
- [11] M. Kusano, H. Ishiduu, , S. Matsummura, and S. Washizu, Expermental study on the reduction of drum brake noise, *SAE paper* 851465, 1985.
- [12] G. D. Liles, Analysis of disc brake squeal using the finite element method, *SAE paper* 891150, 1989.
- [13] H. Ghesquire, and L. Castel, High frequency vibrational coupling between automobile brake disc and pads, *IMechE Autotech 1991*, seminar, paper C/427/11/021.
- [14] H. Ghesquire, Brake squeal noise analysis and prediction, *IMechE Autotech 1992*, seminar, paper C389/257.

- [15] J. Hulten, Some drum brake squeal mechanisms, *SAE* 951280, 1995.
- [16] H. Takata, W. Jiang, and T. Nishi, The theoretical and experimental investigations on drum brake squeal, *Noise-Con 98*, April 5-8, 1998, Ypsilanti, Michigan, USA, 1998.
- [17] G. Adams, Self-excited oscillations in sliding with a constant friction coefficient, DE- Vol. 84-1, 1995 *Design Engineering Technical Conference*, Volume 3- Part A, ASME, 1995.
- [18] J.E. Mottershead, and S.N. Chan, Brake squeal – an analysis of symmetry and flutter instability, Friction – induced vibration, chatter, squeal and chaos, *ASME* 1992, vol. 49, pp. 87-97.
- [19] I.L.M. Ahmed, *Study of the Behavior of the Vehicle Disc Brakes*, Ph.D. Thesis, University of Northumbria at Newcastle Upon Tyne, UK, 2002.
- [20] J. Huang, C.M. Krousgrill, and A.K. Bjjaj, Modelling of automotive drum brakes for squeal and parameter sensitivity analysis, *Journal of Sound and Vibration*, 289 (2006), 245-263, 2006.
- [21] B.K. Servis, *The onset of squeal vibrations in drum brake systems resulting from a coupled mode instability*, Ph.D. Thesis, Purdue University, West Lafayette, IN, 2000.
- [22] J.D. Fieldhouse, and Peter Newcomb, An Investigation Into Disc Brake Squeal Using Holographic Interferometry, *3rd International EAEC Paper* No.91084, Strasborg, June 1991.
- [23] J.M. Lee, S.W. Yoo, J.H. Kim, and C.G. Ahin, A study on the squeal of a drum brake which has shoes of non-uniform cross section, *Journal of Sound and Vibration* (2001), 240(5), 789-808, 2001.
- [24] ANSYS user's Manual.
- [25] ABAQUS user's manual.
- [26] Y.S. Lee, P.C. Brooks, D.C. Barton, and D.A. Crolla, A Study of Disc Brake Squeal Propensity Using a Parametric Finite Element model, *European Conference on Vehicle Noise and Vibration*, IMechE, C521/009/98, 1998.
- [27] A.J. Day, and P.R.J. Harding, Performance variation of cam operated drum brakes, *Proceedings of the IMechE Conference on braking of road vehicles*, 1983, paper C10/83. pp. 69-77.
- [28] Yongbin Yuan, A Study of the Effect of Negative Friction-Speed Slope on Brake Squeal, *ASME Design Engineering Technical Conference* Volume 3- Part A, pp. 1153-1162, 1995.